

# Growth Mechanism of Synthetic Imogolite Nanotubes

Huixian Yang,<sup>†</sup> Cheng Wang,<sup>‡</sup> and Zhaohui Su<sup>\*,†</sup>

State Key Laboratory of Polymer Physics and Chemistry and State Key Laboratory of Rare Earth Resources Utilization, Changchun Institute of Applied Chemistry, Chinese Academy of Sciences, 5625 Renmin Street, Changchun, Jilin 130022, P.R. China

Received January 16, 2008. Revised Manuscript Received March 25, 2008

By controlling the surface effects during droplet evaporation of imogolite solutions, imogolite nanotubes were dispersed individually and directly observed by transmission electron microscopy (TEM), and the structure evolution of imogolite nanotubes in the synthetic process was investigated. It was found that the number of imogolite nanotubes continuously increased with time in the whole reaction. The average length grew slowly over time after a remarkable increase in the initial 24 h, and the length distribution experienced a similar variation with the polydispersity index always below 2. No appreciable changes in tube diameters were detected under TEM observation. The nutrient diffusion controlled kinetic formation mechanism is favored by our semiquantitative analysis of the experimental results. Adding nanotube “seeds” to a fresh reaction solution promoted further growth of the nanotubes. This served as a consolidated support to the proposed kinetic controlled mechanism.

## Introduction

Imogolite is a naturally occurring single-walled nanotubular aluminosilicate with an empirical formula of  $(\text{OH})_3\text{-Al}_2\text{O}_3\text{SiOH}$ . It has an inner diameter of around 1.0 nm, an external diameter of around 2.5 nm, and a length ranging from hundreds of nanometers to micrometer scale. The inner surface of the nanotube is composed of Si-OH groups while the outer surface is Al-OH groups. These hydroxyl groups make the nanotube hydrophilic<sup>1–5</sup> and the positive charges on the outer surface under acidic condition allow the nanotubes to be highly dispersed in water because of electrostatic repulsion. Compared with its close analogue, single walled carbon nanotube (SWCNT), which has received tremendous research interest in the past decade and possesses extensive potential applications due to its superior mechanical, chemical, electrical, and thermal properties,<sup>6,7</sup> imogolite could be easily obtained without using expensive synthetic apparatus and tedious post-separation process. Its composition, structure, synthesis, and applications have been the subject of research for nearly half of a century. Recently, the use of imogolite as filler for organic/inorganic composites, electron emitter, support for nanosized noble metals, and shape-selective catalyst has been attempted.<sup>8–14</sup>

Despite the advancements in both fundamental research and application of this unique inorganic nanotube, the formation of its curved enclosure structure and the growth along the tubular axis remain unclear because of the complexity and sensitivity of the reaction system. Generally imogolite is prepared by mixing aluminum chloride with orthosilicate in aqueous solution. In this process, soluble aluminum ionic species and the hydrolysis of the silicon precursor depend strongly on the pH, which tends to drop during the formation of imogolite. The curvature of the nanotube originates from the difference between bond lengths of the Al–O and Si–O bonds, which are 1.9 and 1.6 Å, respectively.<sup>1</sup> On the basis of NMR, IR, transmission electron microscopy (TEM), and X-ray diffraction (XRD) results, it was proposed that enclosure of protoimogolite, a presumed sheet-like particle, took place in the early stage of the reaction and served as nuclei for the post-growth of imogolite nanotubes. A progressive nucleation and their subsequent growth lead to the increase of nanotube concentration. This scenario can be described as a kinetic based approach for the synthesis of imogolite nanotubes although further direct evidence is needed.<sup>15–17</sup> Recently, after combining mainly TEM observations and dynamic light scattering (DLS) analysis, Nair et al.<sup>4</sup> reported that the average length of imogolite nanotubes remained unchanged at the later stage

\* To whom all correspondence should be addressed. Tel: (86)431-85262854. Fax: (86)431-85262126. E-mail: zhsu@ciac.jl.cn.

<sup>†</sup> State Key Laboratory of Polymer Physics and Chemistry.

<sup>‡</sup> State Key Laboratory of Rare Earth Resources Utilization.

- (1) Cradwick, P. D. G.; Farmer, V. C.; Russell, J. D.; Masson, C. R.; Wada, K.; Yoshinaga, N. *Nat. Phys. Sci.* **1972**, *240*, 187.
- (2) Farmer, V. C.; Adams, M. J.; Fraser, A. R.; Palmieri, F. *Clay Miner.* **1983**, *18*, 459.
- (3) Bursill, L. A.; Peng, J. L.; Bourgeois, L. N. *Philos. Mag. A* **2000**, *80*, 105.
- (4) Mukherjee, S.; Bartlow, V. M.; Nair, S. *Chem. Mater.* **2005**, *17*, 4900.
- (5) Gustafsson, J. P. *Clays Clay Miner.* **2001**, *49*, 73.
- (6) Popov, V. N. *Mater. Sci. Eng. R* **2004**, *43*, 61.
- (7) Moniruzzaman, M.; Winey, K. I. *Macromolecules* **2006**, *39*, 5194.
- (8) Ackerman, W. C.; Smith, D. M.; Huling, J. C.; Kim, Y. W.; Bailey, J. K.; Brinker, C. J. *Langmuir* **1993**, *9*, 1051.

- (9) Imamura, S.; Kokubu, T.; Yamashita, T.; Okamoto, Y.; Kajiwara, K.; Kanani, H. J. *Catalysis* **1996**, *160*, 137.
- (10) Suzuki, M.; Suzuki, S.; Tomura, S.; Maeda, M.; Mizota, T. J. *Ceram. Soc. Jpn.* **2001**, *109*, 874.
- (11) Yamamoto, K.; Otsuka, H.; Takahara, A. *Polym. J.* **2007**, *39*, 1.
- (12) Miyachi, N.; Aomine, S. *Soil Sci. Plant Nutr.* **1966**, *12*, 187.
- (13) Liz-Marzán, L. M.; Philipse, A. P. *J. Phys. Chem.* **1995**, *99*, 15120.
- (14) Oh, J.; Chang, S.; Jang, J.; Roh, S.; Park, J.; Lee, J.; Sohn, D.; Yi, W.; Jung, Y.; Kim, S.-J. *J. Mater. Sci.: Mater. Electron.* **2007**, *18*, 893.
- (15) Barrett, S. M.; Budd, P. M.; Price, C. *Eur. Polym. J.* **1991**, *27*, 609.
- (16) Wilson, M. A.; Lee, G. S. H.; Taylor, R. C. *J. Non-Cryst. Solids* **2001**, *296*, 172.
- (17) Farmer, V. C.; Smith, B. F. L.; Tait, J. M. *Clay Miner.* **1979**, *14*, 103.

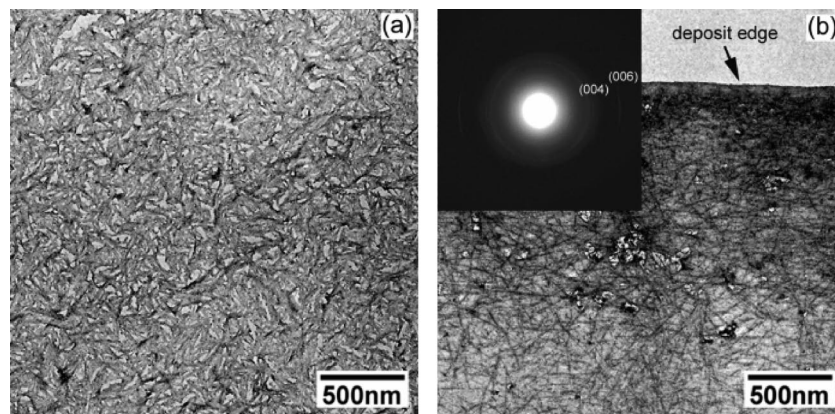


**Figure 1.** BF electron micrographs and corresponding SAED patterns of imogolite at 3 h reaction time, selected from (a) the interior region and (b) the edge region of the deposit pattern.

of the synthesis and proposed that the growth of imogolite nanotubes may be a thermodynamically driven self-assembly process.

In this paper, we employed a synthetic method similar to that used by Nair et al. for the preparation of these inorganic nanotubes but will mainly focus on the post growth process. The impetus of this work is to clarify the currently existing discrepancy on imogolite growth mechanism. Using a newly developed TEM specimen preparation method,<sup>18</sup> dispersed imogolite nanotubes can be directly observed under TEM, which has not been achieved previously. Such direct observation of individually dispersed imogolite nanotubes allows a semiquantitative analysis in terms of the tube numbers and dimensions. On the basis of these results and analysis, a kinetic structure evolution of imogolite nanotubes was proposed, which was further supported by a designed seeded growth experiment.

### Experimental Section

**Synthesis of Imogolite.** Imogolite was prepared following a previous report.<sup>19</sup> Briefly, tetraethoxysilane [Si(OEt)<sub>4</sub>] was added dropwise to 2.4 mmol/L aluminum chloride (AlCl<sub>3</sub>·6H<sub>2</sub>O) aqueous solution to achieve 1.8 Al:Si ratio. The pH of the solution was first increased to 5.0 using 0.1 mol/L sodium hydroxide aqueous solution to allow the hydrolysis of the precursors, and then the solution was acidified by adding 1.0 mmol of hydrochloric acid and 2.0 mmol of acetic acid per liter of the solution. The acidified solution was then refluxed at 98 ± 2 °C for 5 days. Solution samples were extracted at various reaction times and dialyzed against deionized water (18.2 MΩ·cm) to remove unreacted silicic acid, monomeric aluminum, and NaCl. The drying of a diluted reaction solution droplet in the ethanol environment was performed by evaporating the droplet on a carbon-coated Formvar copper grid in saturated ethanol vapor. To achieve semiquantitative analysis, the diameters of all droplets were controlled through applying the same volume of dialyzed reaction solution on the grids. For comparison, a droplet of the dialyzed solution (at 3 and 120 h reaction time, respectively) was deposited onto the grid and then dried in air at ambient conditions.

**Electron Microscopy.** TEM observations were carried out on a JEOL 1011 microscope operating at 100 kV. The camera length was calibrated with Au standard.

### Results and Discussion

When using a normal specimen preparation method, only entangled imogolite networks could be observed under TEM. Figure 1 shows two bright field (BF) electron micrographs of the synthetic product obtained after 3 h of reaction. These two micrographs were captured from different regions of the same deposit pattern. In the interior region, no evidence of imogolite nanotubes could be traced and only amorphous agglomerates are observed (Figure 1a). However, a small amount of nanotubes is clearly visible in the edge region of the deposit (Figure 1b). The characteristic (004), (006) reflection arcs (inset of Figure 1b), corresponding to the periodic repeat unit along the imogolite nanotube axis, well support the formation of imogolite nanotubes at this time and indicate a partially ordered nanotube array in this region. The amorphous agglomerates, which probably are the dried solutes, are the dominant products residing evenly in the deposit pattern.

The dramatic difference between the morphology shown in the two micrographs is the consequence of uneven distribution and accumulation of synthetic products in the droplet drying process. Deegan et al.<sup>20,21</sup> proposed that in drying a droplet of colloidal solution on substrate, the pinned contact line causes capillary flow toward the edge of the drop, and the solutes are then delivered to the perimeter of the drop by this flow and accumulate there to form a ring-like deposit. Here due to the shape anisotropy, imogolite nanotubes are liable to align along the fluid flow direction during droplet evaporation. When drying a drop of imogolite solution obtained from early stage of the reaction, the nanotubes are delivered to the edge of the drop by radial capillary flow and retain the alignment after the water evaporates. Small amounts of the nanotubes are more easily observed near the edge region of a deposit than in the interior region. In addition, the ordered alignment of the nanotubes along the deposit edge is attributed to the geometrical constraint effects in the pinning evolution of the droplet drying process. This probably was the reason that no

(18) Yang, H.; Su, Z. *Chin. Sci. Bull.* **2007**, *52*, 2301.

(19) Farmer, V. C.; Fraser, A. R.; Tait, J. M. *J. Chem. Soc., Chem. Commun.* **1977**, *13*, 462.

(20) Deegan, R. D.; Bakajin, O.; Dupont, T. F.; Huber, G.; Nagel, S. R.; Witten, T. A. *Phys. Rev. E* **2000**, *62*, 756.

(21) Deegan, R. D.; Bakajin, O.; Dupont, T. F.; Huber, G.; Nagel, S. R.; Witten, T. A. *Nature* **1997**, *389*, 827.

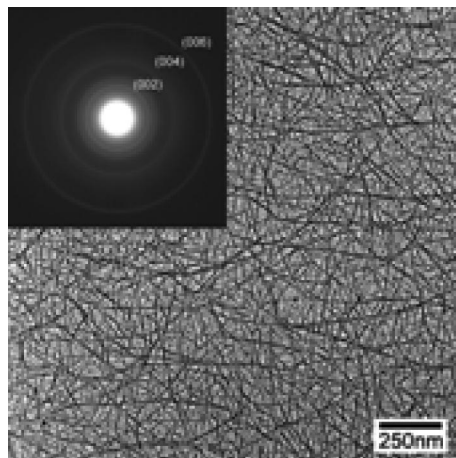


**Figure 2.** BF electron micrograph and corresponding SAED pattern of imogolite at 120 h reaction time.

imogolite nanotube formation was reported at an earlier reaction stage, such as less than 10 h reaction time.<sup>4</sup>

When the reaction time was prolonged to 120 h, imogolite nanotubes could be observed as a dense entangled network spread everywhere on the grid (Figure 2). The result coincides with previous findings, indicating the remarkable quantity increase of imogolite nanotubes in the reaction solution. However, similar to the results obtained at early stage (Figure 1), the exact length of the imogolite nanotubes can not be extracted from the TEM data. To surmount such obstacle in observing imogolite nanotubes under TEM, recently we developed a specimen preparation method for imogolite<sup>18</sup> by taking advantage of surface effects in the droplet drying process. Instead of drying the TEM specimen at ambient conditions, the carbon-coated Formvar copper grid with a droplet of dialyzed imogolite aqueous solution was allowed to dry in saturated ethanol atmosphere. In this case, the proportion of evaporation from the droplet perimeter is greatly reduced, and the solution evaporates approximately spatially uniform along the droplet surface.<sup>20–22</sup> Moreover, the dissolution of ethanol in water decreases the surface energy of the droplet, which restrains the nanotubes from aggregating to form entangled bundles and makes the individual dispersion of the nanotubes on the substrate possible.

With this TEM specimen preparation method, direct observation of individual imogolite nanotubes with definite dimensions could be achieved. It also makes the investigation of the growth process of the nanotubes possible as the concentration and the exact length of the nanotubes can be quantitatively analyzed through our controlled experiments. Figure 3 shows the BF electron micrographs of the imogolite nanotubes obtained at 1 h, 3 h, 9 h, 24 h, 37 h, and 120 h reaction time. Since the concentration of the imogolite nanotubes was rather high at 120 h, the extracted solution was diluted by 50 times with deionized water and the same volume of the diluted dispersion was applied to the grid. As seen in Figure 3a, a small number of the nanotubes with a diameter of  $\sim 2.5$  nm could be discerned out of the

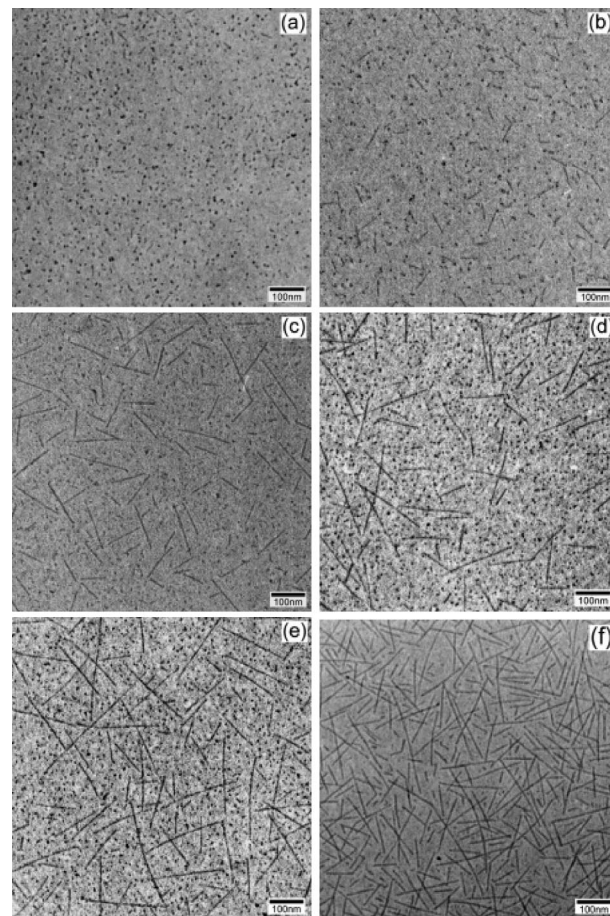


**Figure 3.** BF electron micrographs of imogolite at reaction time of (a) 1 h, (b) 3 h, (c) 9 h, (d) 24 h, (e) 37 h, and (f) 120 h. Specimens were prepared by droplet evaporation of the imogolite solution in ethanol atmosphere.

amorphous product, indicating the formation of imogolite nanotubes at as early as 1 h reaction. The lengths of the nanotubes are below approximately 50 nm. The direct observation of imogolite nanotube formation at so early a stage had not been achieved in previous reports using normal TEM specimen preparation method. For the rest of the micrographs in Figure 3, the concentration of the imogolite nanotubes increases with reaction time, especially in the first 24 h, and the length of the nanotubes falls into a fairly large range. It should be noted that the diameter of the nanotubes remains almost unchanged throughout the synthesis.

On the basis of the experimental results shown in Figure 3, a quantitative analysis for the concentration and average length of the imogolite nanotubes was carried out. Three areas of  $1.0 \times 1.0 \mu\text{m}^2$  for each specimen were analyzed to ensure what we observed under TEM were representative of imogolite in the solution. The numbers of the imogolite nanotubes were counted, and the length of each nanotube was measured for each  $1.0 \times 1.0 \mu\text{m}^2$  area. The dependence of the averaged numbers of the nanotubes among three areas on reaction time is presented in Figure 4a. The error bar represents the standard deviation among the three replicates. Clearly, this number enhances rapidly in the first 9 h and then shows a nearly linear increase with a lower slope for the rest of the reaction until 120 h. This trend is consistent with the qualitative observations reported previ-

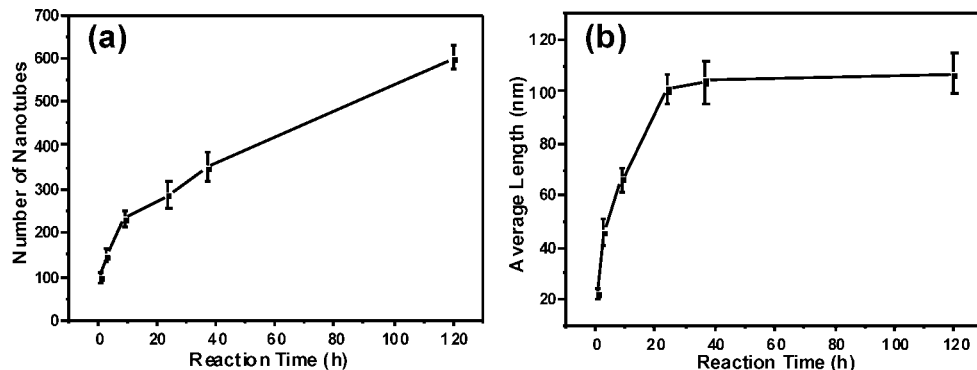


Figure 4. Dependence of (a) the numbers and (b) the average lengths of imogolite nanotubes on the reaction time.

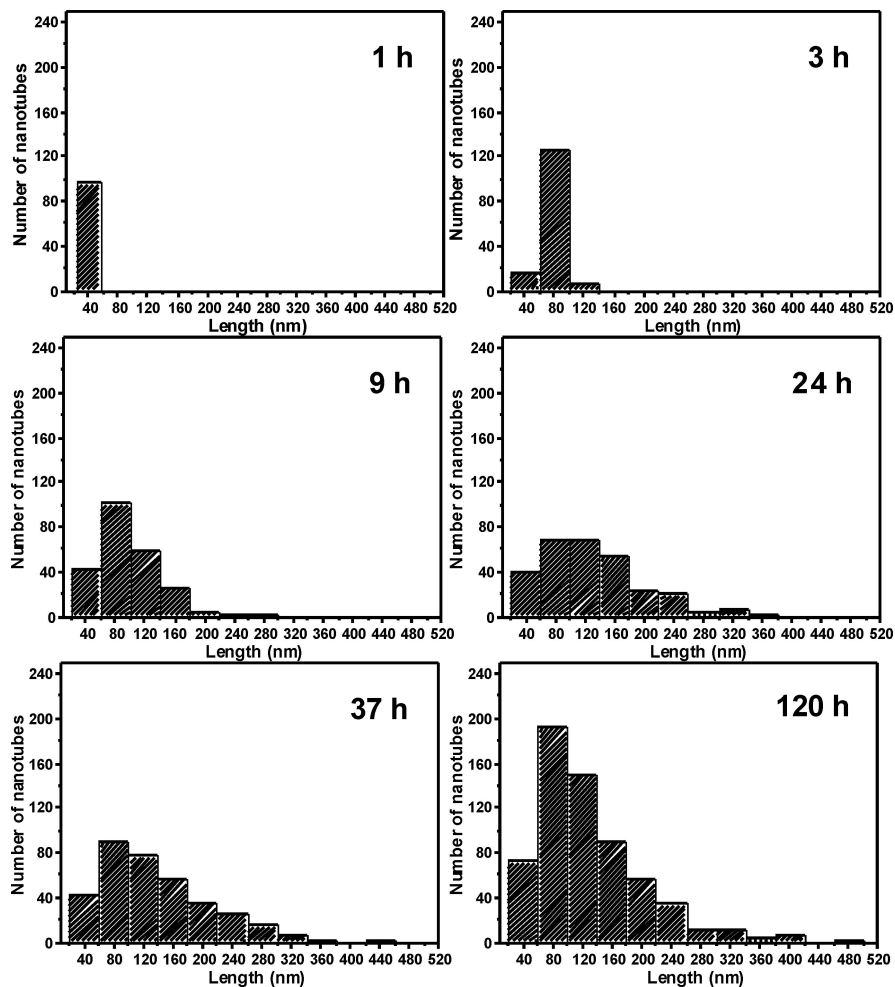


Figure 5. Length distribution of synthetic imogolite nanotubes at different reaction times.

ously.<sup>1,3,4,8,15,16</sup> Figure 4b gives the average lengths of the imogolites varying with the reaction time. The average length increases dramatically in the early stage of the reaction, from 22 nm at 1 h to 101 nm at 24 h, and reaches a nearly stable stage after that. However, imogolites with length longer than 100 nm tend to appear when the reaction time was prolonged to more than 3 h, as seen in Figure 5, which shows the length distribution for the nanotubes observed in the area investigated. Short nanotubes with length below 50 nm are formed within 1 h of reaction. More than half of the nanotubes have their lengths falling into the 50–100 nm range only 2 h later. Although some long nanotubes are formed at longer reaction time, the dominant products are still short nanotubes with

their length around and below 100 nm. For these cases, however, the increases of the average lengths were canceled out by the continuous formation of new short imogolite nanotubes.

The phenomenon that the *average* lengths of imogolite nanotubes remain nearly unchanged when the reaction time is longer than 24 h was also revealed in Nair's report using DLS to measure the tube lengths.<sup>4</sup> On the basis of the DSL results, they proposed a thermodynamically driven self-assembly mechanism. As an indirect means for characterizing particle dimensions, DLS yields statistical results for this purpose and only the *average* lengths could be obtained. The growth trend they reported for the average length of imogolite

**Table 1. Polydispersity Index (PDI) of Synthetic Imogolite Nanotubes at Various Reaction Times**

reaction time (h)	polydispersity index (PDI)
1	1.09
3	1.13
9	1.37
24	1.45
37	1.52
120	1.52

nanotubes is similar to what we found here by direct TEM observation. Prior to this thermodynamic mechanism, kinetic growth was believed to play a major role in the imogolite nanotube formation, although no convincing evidence was provided. According to this kinetic mechanism,<sup>16,17</sup> the “protoimogolite” precursors appear early in the reaction and provide nuclei for the growth of the nanotubes by polymerization, and the tube length increases with reaction time by addition of the precursors to the growing ends of the tubes. This growth mechanism is consistent with what has been observed in the initial 24 h of the synthesis, where the numbers and the average lengths of the nanotubes rapidly increase with reaction time. However, intuitively it seems to contradict with the observation that the *average* lengths of the imogolite (appears to remain constant<sup>4</sup> or) only increase slightly in the later stage of the synthesis as we found. Detailed analysis of the numbers, lengths, and length distributions of the imogolite nanotubes indeed supports this mechanism. As can be seen in Figure 5, the addition of precursors to the growing ends of the tubes, which leads to the length increase of individual nanotubes, does not cease even when the reaction times are 37 and 120 h. This means that the longer nanotubes continue to grow along the synthetic course, as predicted by the kinetic growth mechanism. This observation does not favor the thermodynamic self-assembly mechanism proposed by Nair et al., where the growth of imogolite nanotubes would be terminated at certain stages.<sup>4,23</sup> The continued growth of the nanotubes is countered by the formation of new short imogolites as a result of progressive nucleation, shown in Figure 4a as the increase of the total number of the nanotubes, and therefore the overall *average* length of the product does not increase dramatically. In addition, progressive addition of nutrients would lead to an expansion of the size distribution over time, which can be clearly verified by examining the polydispersity index (PDI) for the tube length at different reaction times as listed in Table 1. In this table, all the PDIs are below 2 despite the remarkable length increase in the initial 24 h. This narrow polydispersity of the tube length may be difficult to detect by techniques such as light scattering in solution.

The kinetic nutrient addition growth mechanism was further tested by a designed “seeded growth” experiment. Such a method has been reported in the literature for the synthesis of imogolite nanotubes; however, no further information about the dimensions of the resulting nanotubes was provided.<sup>8</sup> Here, a small amount of synthetic imogolite nanotubes (10 wt %), which was obtained after 120 h of

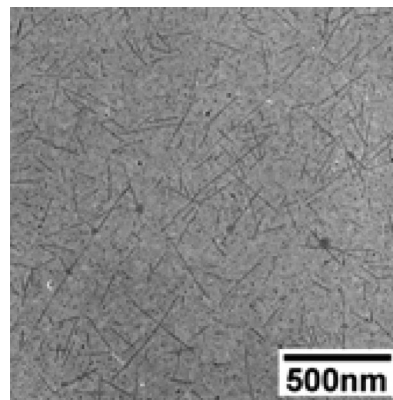


**Figure 6.** BF electron micrograph of “seeded” imogolites after 120 h reaction time; the population of long nanotubes is significantly higher.

reaction, was added as “seeds” to a fresh precursor solution and the reaction was allowed to proceed for another 120 h. The TEM micrograph shown in Figure 6 reveals that some of nanotubes can grow to longer than 500 nm, which are rarely found in the one-batch synthesis process. This result confirms that the growing ends of the long tubes remain reactive and can continuously grow even with lower mobility.

## Conclusions

In the present work, we have investigated the growth process of imogolite nanotubes from precursors in aqueous solution by TEM, and the lengths of the tubes at various reaction times have been directly measured and analyzed. Imogolite nanotubes appear after 1 h of growth, much earlier than previously reported, and the tube diameters remain constant and monodisperse while the tube lengths are polydisperse throughout the whole process. The process can be described as a kinetic nutrient addition growth mechanism. At the beginning protoimogolites and short imogolites are formed and grow quickly, resulting in a rapid increase in both the number and the average length of the nanotubes. The substantial growth of the tube length and the concentration increase make the solution more sluggish, and the overall reaction slows down. In the later stage of the growth process, the polymerization is mainly through the formation of new nanotubes and the growth of shorter tubes, which leads to continuous increase in the number and total mass of the imogolite nanotubes and a relatively constant average tube length. The length distribution remains narrow with the polydispersity index well below 2. Moreover, the nanotubes synthesized can continue to grow much longer in a fresh precursor solution, indicating that the ends of the imogolite nanotube stay open and active. These findings may help chemists synthesize inorganic nanotubes with precise dimensions designed for photonics and other applications.

**Acknowledgment.** This work was supported by the National Natural Science Foundation of China (20423003, 20774097) and the National Basic Research Program of China (2007CB925101, C.W.). Z.S. thanks the NSFC Fund for Creative Research Groups (50621302) for support.